International Journal of Rock Mechanics & Mining Sciences 70 (2014) 82–89

Contents lists available at ScienceDirect

International Journal of Rock Mechanics & Mining Sciences

journal homepage: www.elsevier.com/locate/ijrmms

Technical Note

Stochastic reconstruction of Gosford sandstone from surface image

Peijie Yin, Gao-Feng Zhao *

Centre for Infrastructure Engineering and Safety, School of Civil and Environmental Engineering, University of New South Wales, Sydney, NSW 2052, Australia

ARTICLE INFO

Article history:
Received 4 October 2013
Received in revised form
1 March 2014
Accepted 25 April 2014

1. Introduction

Most rocks have complex microstructures, which are regarded as the most important factor in determining their mechanical properties and transport behaviors [1,2]. Moreover, to obtain the microstructure of material is one of the intrinsic interests of scientists. For instance, two Nobel Prizes were awarded for the inventions of X-ray Computed Tomography (CT) and Scanning Electron Microscope (SEM). In geosciences and geomechanics, these devices have been used to obtain the microstructure of geomaterials for different purposes, e.g. the study of fracturing in granite by Ichikawa et al. [3], the investigation of thermally induced microcracks in concrete by Wang et al. [4], the characterization of shale rock properties by Josh et al. [5], and the analysis of energy dissipation in Gosford sandstone by Sufian and Russell [6]. However, the SEM and X-ray CT are not perfect, besides being expensive and time consuming, there are limitations. The SEM can only get the surface image, and the X-ray CT is usually only applicable to small-size specimens when the resolution is high.

Recently, a possible solution has been developed to reconstruct the microstructure model of a porous media based on its morphological information, and it is called stochastic reconstruction [7]. The stochastic reconstruction is capable to reproduce a large number of microstructure models for a material at little cost. Moreover, using the method, it is possible to generate a microstructure model of large size under high resolution. The principle of the stochastic reconstruction is straightforward and easy to understand. The reconstruction is treated as an optimization problem where the microstructure model is the target variable and the difference between the morphological description curves of the target material and the reconstructed microstructure model serves as the target function. The goal is to find the best solution to minimize the target function. The simulated annealing method has been widely used as an optimization method [7–9], and the two-point probability function, lineal path function, and multiple-point statistics function are commonly adopted as the morphological descriptor [10–13]. Stochastic reconstruction has been used to generate microstructure models of different materials, e.g. dispersions by Rintoul and Torquato [14], Berea and Fontainebleau sandstones by Manwart et al. [15], chalk by Talukdar and Torsaeter [16], and other heterogeneous materials by Jiao et al. [17]. However, in these works, the morphological description curve is simply obtained from 2D images of the corresponding material [9,16–19]. Whether the morphological description curve can reflect the 3D morphological information of the target material is not verified. Moreover, the reconstructed microstructure models have not been validated against the real microstructure of the material.

In this paper, the stochastic reconstruction is adopted to generate the microstructure model of the Gosford sandstone. The proposed method is illustrated in Fig. 1. The surface image of the Gosford sandstone is captured using a digital microscope. The relationship between the morphological description curves of the 2D image and the 3D model is studied based on the X-ray micro-CT data of the Gosford sandstone. Then, the simulated annealing method is used to generate the microstructure of the Gosford sandstone. The reconstructed models are compared with the X-ray micro-CT model. The main contributions of the present work are: the employment of a digital microscope to obtain the surface image; the derivation of the 3D morphological distribution curve from the 2D surface image, and the verification of the reconstructed microstructure model. From our study, it is concluded that the stochastic reconstruction procedure is reasonably good to generate the microstructure model for Gosford sandstone.

* Corresponding author. Tel.: +61 2 9385 5022; fax: +61 2 9385 6139.
E-mail address: gaofeng.zhao@unsw.edu.au (G.-F. Zhao).

http://dx.doi.org/10.1016/j.ijrmms.2014.04.012
1365-1609/

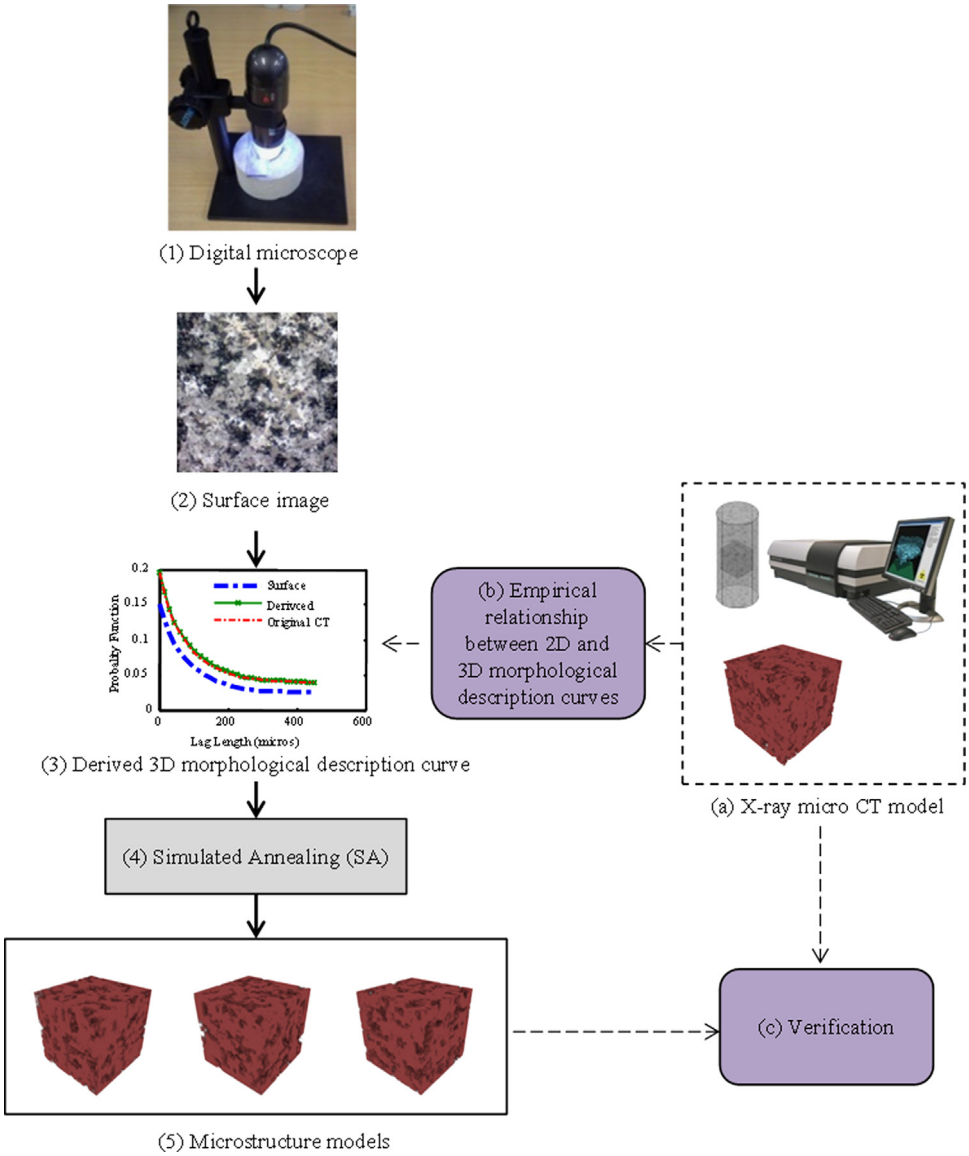

Fig. 1. Illustration of the stochastic reconstruction for Gosford sandstone.

2. Stochastic reconstruction

2.1. Two-point probability function

In this paper, the porous media is considered as a two-phase mixture consisting of the solid and pores, and it is represented by a binary phase function $I(\vec{r})$ as

$$I(\vec{r}) = \begin{cases} 1, & \vec{r} \text{ is in the pore phase} \\ 0, & \vec{r} \text{ is in the solid phase} \end{cases} \quad (1)$$

where $\vec{r}$ is the spatial position of a point in the porous media.

The two-point probability function is the most widely used morphological descriptor in the stochastic reconstruction, which is written as

$$S_2(\vec{r}_i, \vec{r}_j) = \langle I(\vec{r}_i) \cdot I(\vec{r}_j) \rangle \quad (2)$$

where $\langle\ \rangle$ denotes the statistical average (probability) of two points in the pore phase at positions $\vec{r}_i$ and $\vec{r}_j$. For a macroscopically homogeneous and isotropic porous media, $S_2(\vec{r}_i, \vec{r}_j)$ only depends on the length, u, of the lag vector $\vec{u} = \vec{r}_j - \vec{r}_i$ between the two points. Thus, the two-point distribution function can be further simplified as

$$S_2(u) = \langle I(\vec{r}_i) \cdot I(\vec{r}_i + \vec{u}) \rangle \quad (3)$$

In the stochastic reconstruction, a porous media is usually represented by a digitalized model. The two-point distribution function of a digitalized model can be calculated as

$$S_2(u) = \frac{\sum\sum I(\vec{r}_i) \cdot I(\vec{r}_i + u\vec{e}_j)}{D\prod L_i} \quad (4)$$

where $\vec{r}_i$ represents a pixel in the interested domain, u is length of the lag vector, $\vec{e}_j$ is the unit vector, D is the dimension of the porous media, and L_i is the size of the domain (in pixels). It should be mentioned that when the periodic boundary condition is considered, the second pixel $(\vec{r}_i + u\vec{e}_j)$ will return to the start boundary $(\vec{r}_i + u\vec{e}_j - L_{j*})|_{j=j*}$ when the point moves beyond the end boundary, with the same normal direction $\vec{e}_{j*}$

The two-point probability function $S_2(u)$ can be viewed as a curve that represents certain morphological information for a porous media. In stochastic reconstruction, the two-point probability function is widely used due to its ease of implementation and high computational efficiency. In this paper, it is adopted as

the morphological descriptor for the reconstruction. There are also other available morphological functions for stochastic reconstruction, and details can be found in, for example, [8,9,12,13].

2.2. Stochastic reconstruction based on the simulated annealing method

The procedure of stochastic reconstruction based on the simulated annealing method is briefly introduced as follows. The target function is defined as

$$E = \sum_{u=0}^{u_{\max}} (\tilde{S}_2(u) - S_2(u))^2 \tag{5}$$

where E is the system energy, $S_2(u)$ is the morphological distribution curve (two-point probability function) of the reconstructed model, $\tilde{S}_2(u)$ is the morphological distribution curve of the target material, and $u_{\max}$ is the maximum lag length which can be determined by accounting the size of the interested domain, the accuracy of the morphological representation and the computational efficiency. In this work, it is taken as one to two tenths of the size of the domain.

There are two stages of iterations in the stochastic reconstruction. The first one is the internal phase exchange based on the Metropolis algorithm without updating of the system temperature:

$$p = \begin{cases} 1, & \Delta E \le 0 \\ e^{-\Delta E/k_B T}, & \Delta E > 0 \end{cases} \tag{6}$$

where p is the probability of accepting the exchange, ΔE is the change of system energy due to the phase exchange, k_B is Boltzmann's constant, and T is the temperature of the current system.

The second one is the Markov chain iteration, which updates the system temperature according to

$$T = T_0 e^{(\lambda-1)(m+1)} \tag{7}$$

in which T_0 is the initial temperature of the system, λ is the reduction parameter of the system temperature and m is the current number of Markov chain. The reduction parameter λ is estimated by

$$\lambda = Max\left[\lambda_{\min}, Min\left(\lambda_{\max}, \frac{E_{\min}}{\overline{E}}\right)\right] \tag{8}$$

where $\lambda_{\min} = 0.2$, $\lambda_{\max} = 0.8$, and $E_{\min}$ and $\overline{E}$ are the minimum and average energy in each Markov chain, respectively.

The Markov chain number m is given by

$$m = N/Ne \tag{9}$$

where N is the total number of iterations, and Ne is Markov chain length which has significant influence on the convergence. For the reconstruction of geomaterials, Ouenes et al. [20] suggested that Ne should be 100 to 300. In this paper, $Ne = 200$ is used.

Generation of the initial model is as described as follows. The first step is to generate a random model with the specific porosity. The phase properties of two pixels are randomly exchanged and the probability of accepting the exchange is p_0. The exchange is repeated for N_0 times. Then, the initial temperature can be calculated as

$$T_0 = -\frac{\Delta E_{\text{sum}}}{N_0 In(p_0)} \tag{10}$$

With the initial model and its parameters ready, the model is iterated until the system energy is less than a specified value, e.g. 1×10^{-5}. Therefore, the morphological curve of the reconstructed model approaches the target one, which guarantees that the reconstructed model has similar morphological information as the target material. More details on the implementation and determination of parameters in the stochastic reconstruction based on simulated annealing method can be found in [16].

3. Quantitative morphological measurements of porous media

3.1. Porosity and specific surface

In stochastic reconstruction, the porosity φ is defined as the probability of finding a point in the pore phase. It also can be represented as the first statistical moment of the phase function $I(\vec{r})$ and is equal to the two-point probability function when $u = 0$.

$$\varphi = S_2(0) \tag{11}$$

Another relationship between the porosity and the two-point probability function is [8]

$$\varphi^2 = S_2(\infty) \tag{12}$$

The specific surface, s, is defined as the interfacial area per unit volume between the two phases. It can be used to evaluate how accurately the pore-solid interface has been reproduced. In the stochastic reconstruction, the specific surface is calculated as [9]

$$s = \frac{-(d/du)S_2(u)|_{u=0}}{2D} \tag{13}$$

where D is the dimension of the reconstructed model.

3.2. Local porosity distribution

The local porosity of the reconstructed model is defined as the porosity within a cubic box of side length l centered at position $\vec{r}$. It is given as

$$\varphi(\vec{r}, l) = \langle I(\vec{r}) \rangle_M \tag{14}$$

where M refers to the operation domain, which is of the size $[i-l/2, i+l/2], [j-l/2, j+l/2], [k-l/2, k+l/2]$ when the measurement box is centered at $\vec{r} = (i, j, k)$. To achieve statistically accurate portrait of the local porosity distribution, the measurement box is moved from left top corner ($l/2$, $l/2$, $l/2$) to right bottom corner ($L_x - l/2$, $L_y - l/2$, $L_z - l/2$) by one pixel each time. Then, the local porosity distribution for a box with a side length of l is evaluated by dividing the number of boxes with porosity in a certain interval $(\varphi, \varphi + \Delta\varphi)$ by the total number of boxes. The local porosity distribution function can be described by [16]:

$$\mu(\varphi, l) = \frac{1}{n} \sum_{\vec{r}} \delta(\varphi - \varphi(\vec{r}, l)) \tag{15}$$

where

$$\delta(\varphi - \varphi(\vec{r}, l)) = \begin{cases} 1, & if\ |\varphi - \varphi(\vec{r}, l)| \le \Delta\varphi \\ 0, & \text{otherwise} \end{cases} \tag{16}$$

and n is the total number of measurement boxes.

3.3. Local percolation probability

In stochastic reconstruction, the local percolation probability is defined as the probability of finding a cubic measurement cell $M_o(\vec{r}, l)$ that percolates in orientation, o. It is expressed as [21,22]:

$$P_o(l) = \frac{1}{n} \sum_{\vec{r}} \Lambda_o(\vec{r}, l) \tag{17}$$

where

$$\Lambda_o(\vec{r},l)=\begin{cases}1, & \text{if } M_o(\vec{r},l) \text{ percolates}\\ 0, & \text{otherwise}\end{cases} \tag{18}$$

The function $\Lambda_o(\vec{r},l)$ can be evaluated using a burning algorithm. First, a fire is set at the pore pixel; the fire then propagates to the neighboring pixel where pore pixel is presented; finally, the fire distinguishes until no neighboring pore pixel can be detected. The process is repeated until all the pore pixels are visited. When the burning process is completed, all the pore clusters are labeled with different fire numbers. The measurement cell is percolated in orientation o if the same cluster numbers are found on opposite sides of the measurement cell in direction o. It means that there exists a path within the cell along orientation o. After all the measurement cells have been visited, the local percolation probability can be measured by using Eq. (17).

4. Morphological description of the Gosford sandstone

4.1. Relationship between 2D and 3D morphological descriptions

X-ray micro-CT scanning with a spatial resolution of 5 μm was conducted on the Gosford sandstone by Sufian and Russell [6]. As shown in Fig. 2, a spatial cube of $600\times600\times600$ pixels ($3\times3\times3$ mm^3) is extracted from the original X-ray micro-CT model by Sufian and Russell [6], which is used to investigate the relationship between 2D and 3D morphological description curves of the Gosford sandstone. The binaryzation of the X-ray micro-CT data is done by adjusting the threshold value based on the porosity of the Gosford sandstone which is reported as 19% [6]. The areal porosity of each 2D CT slice image is shown in Fig. 3. The areal porosity of the CT slice is mostly different from the 3D porosity. The morphological description curves of 2D and 3D models are also different (see Fig. 4). It is found that the morphological description curve of a 2D slice image is close to that of the 3D model when the areal porosity is near the 3D porosity. Therefore, the specific surface image with areal porosity equal to the 3D porosity can be used to extract the 3D morphological description

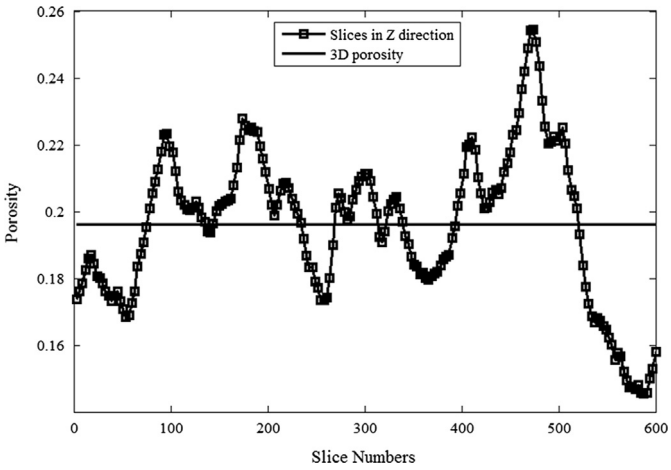

Fig. 3. Areal porosity distribution of the X-ray micro-CT model.

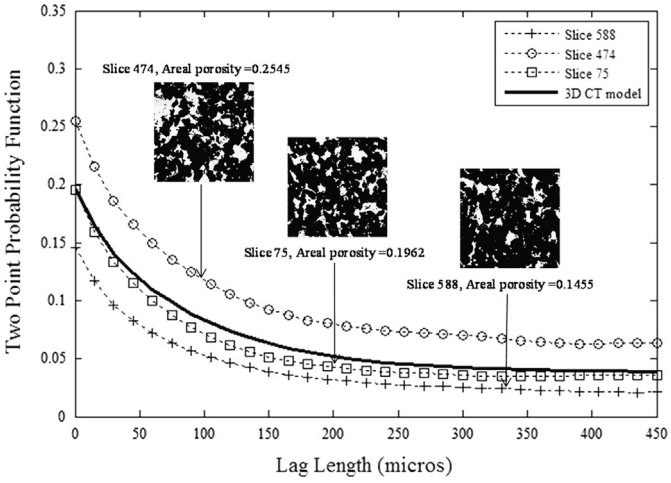

Fig. 4. Morphological description curves of different CT slices.

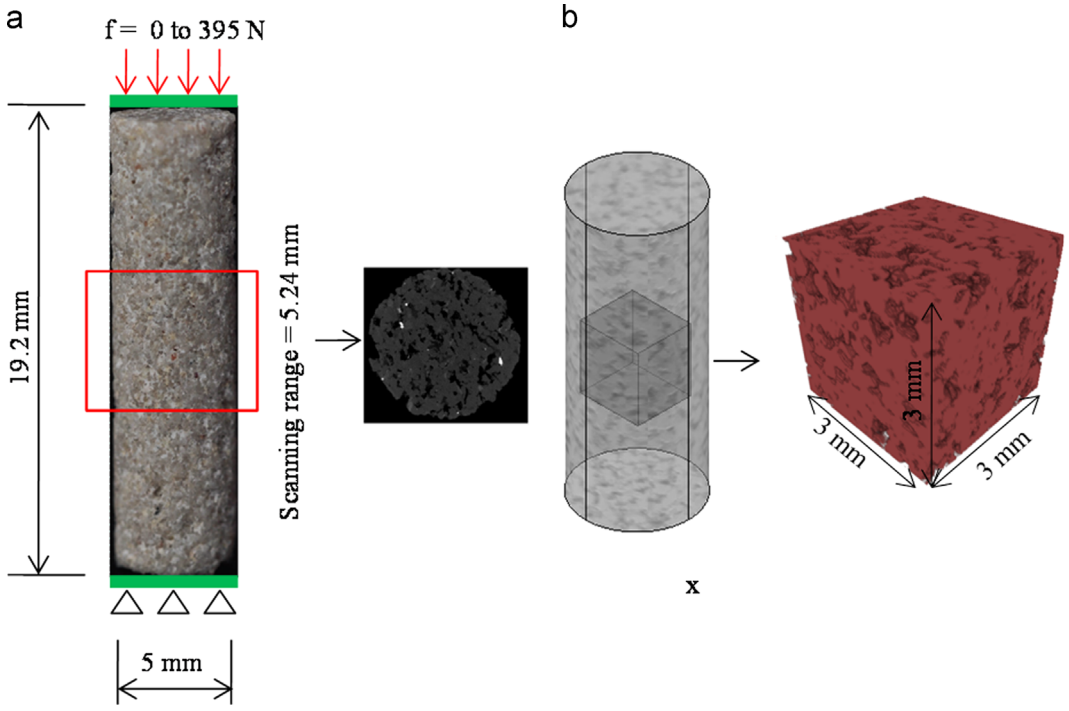

Fig. 2. Sample drilled for X-ray micro-CT scanning and region of interests selected for analysis. (a) Gosford sandstone specimen [6] and (b) X-ray micro CT model.

curve for the stochastic reconstruction. However, it is difficult to find this specific image in practice. One alternative solution is to modify the areal porosity by adjusting the threshold value if the surface image is in a gray format. The rough range of the threshold value is usually determined between two peaks of the histogram of the gray values, e.g., [16]. However, in their work, the morphological description curve from the slice image is simply adopted for reconstruction without further comparison with the corresponding 3D one. To quantify the difference between the 2D and 3D morphological description curves, an index, Ω, in the same form as the system energy in the stochastic reconstruction is used:

$$\Omega = \sum_{u=0}^{u_{\max}} (S_2^{3D}(u) - S_2^{2D}(u))^2 \tag{19}$$

To verify the method, the original CT slice images with the highest and lowest porosities as shown in Fig. 4 are processed. The results are presented in Fig. 5, which prove the applicability of the method. In this method (named method 1), only the porosity and 2D image of the porous media are required, and they are easy to obtain. The shortcoming is that changing the areal porosity of a surface image may influence its original morphological information. For instance, if a surface image with low areal porosity is adjusted to a very high porosity binary image, more pores will be generated and connectivity between pores will be influenced as well. Moreover, the method is not applicable when the surface 2D image is already in the binaryzation form.

Another solution is introduced, which is called method 2 in this paper. According to Eqs. (11) and (12), we have

$$S_2^{3D}(0) - S_2^{2D}(0) = \varphi_{3D} - \varphi_{2D} \tag{20}$$

$$S_2^{3D}(\infty) - S_2^{2D}(\infty) = \varphi_{3D}^2 - \varphi_{2D}^2 \tag{21}$$

If u_{max} is large enough, the following relationship stands

$$S_2^{3D}(u_{\max}) - S_2^{2D}(u_{\max}) \doteq \varphi_{3D}^2 - \varphi_{2D}^2 \tag{22}$$

Then, the relationship between 2D and 3D morphological distribution is assumed to satisfy the following equation

$$S_2^{3D}(u) = S_2^{2D}(u) + (\varphi_{3D} - \varphi_{2D})w(u) + (1 - w(u))(\varphi_{3D}^2 - \varphi_{2D}^2) \tag{23}$$

where $w(u)$ is the weight function which is estimated from the normalized 2D correlation function as

$$w(u) = \frac{S_2^{2D}(u) - S_2^{2D}(u_{\max})}{S_2^{2D}(0) - S_2^{2D}(u_{\max})} \tag{24}$$

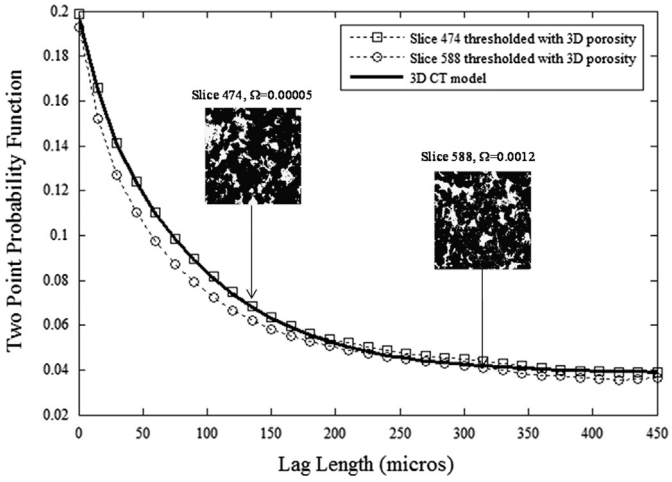

Fig. 5. Derived morphological description curves of the CT slices (method 1).

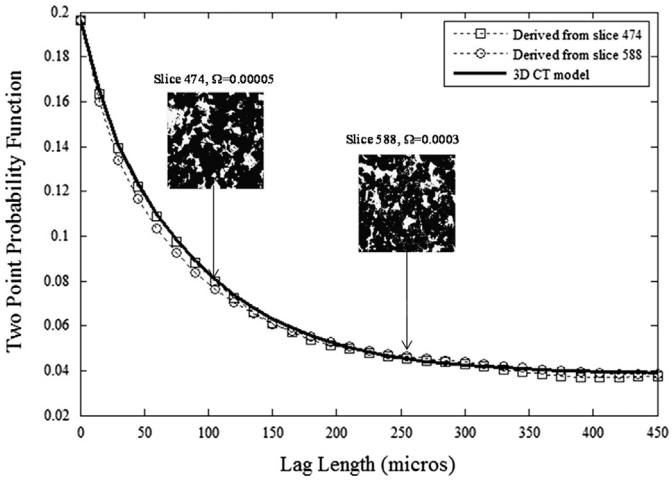

Fig. 6. Derived morphological description curves of the CT slices (method 2).

Eq. (23) can directly derive the 3D morphological distribution curve from the 3D porosity. The merit of method 2 is that no digital image processing is required, and the binarized slice image can also be used. Fig. 6 shows that the derived 3D morphological distribution curves for the binarized slice images are close to the 3D one, which shows the effectiveness of method 2.

4.2. Surface image of the Gosford sandstone

A digital microscope with a magnification ratio up to 600× is used to capture the surface image of a Gosford sandstone specimen (see Fig. 7a). The top surface of the specimen is milled into a flat plane. Carbon dust is poured to fill the pores, and redundancy dust is wiped off the surface to give a processed surface (see Fig. 7c). The carbon dust treatment can decrease the influence of mineral components on pore identification, and is necessary to obtain the 2D porosity structure. Fig. 7e shows the surface image obtained from the digital microscope. The pixel resolution is 5.5 μm, which is fairly good compared to the X-ray micro-CT scanning used in [6]. It should be mentioned that the cost for a digital microscopy is only about 50 Australian dollars.

Four surface images of the Gosford sandstone specimen are captured (see Fig. 8). The region of interest is 3×3 mm^3. The 3D morphological description curves from these images are derived by using the two methods presented in Section 4.1. The discrepancies between the derived curve and that from the X-ray micro-CT model are shown in Table 1. Both methods can provide a reasonable 3D morphological description for the Gosford sandstone. It should be mentioned that the surface of the Gosford sandstone specimen may be partially damaged during the milling process. The results in Table 1 show the robustness of the method in acquiring the morphological description of the Gosford sandstone.

5. Stochastic reconstruction of the Gosford sandstone

5.1. Reconstruction based on the X-ray micro-CT model

In this section, the morphological distribution curve obtained from the X-ray micro-CT model is used. Four reconstructed models are shown in Fig. 9. The stochastic reconstruction can reproduce models for different microstructures with local porosity distribution and local percolation probability close to the original X-ray micro-CT model (see Fig. 10). To quantify the difference between

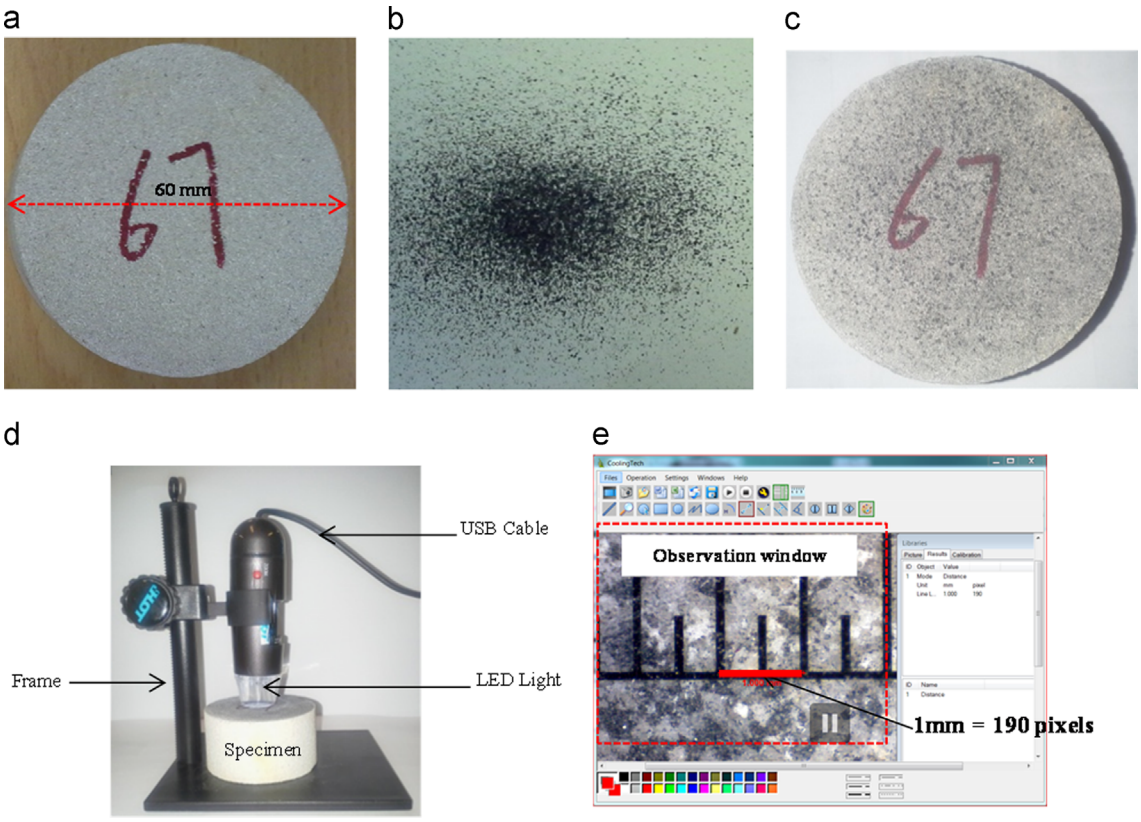

Fig. 7. Process of the surface image acquisition for the Gosford sandstone. (a) Sandstone specimen, (b) Carbon dust, (c) Surface filled with Carbon dust. (d) S04-600X Digital Microscope and (e) Microscope of the specimen surface.

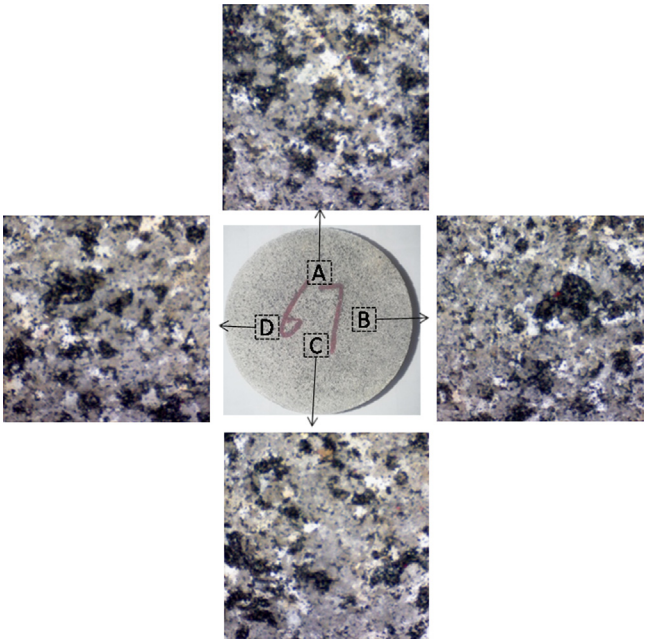

Fig. 8. Obtained surface images of the Gosford sandstone specimen.

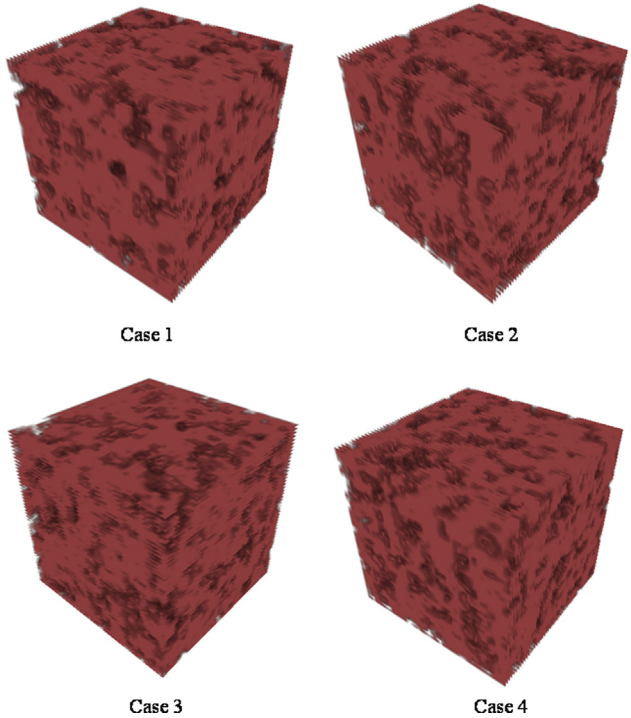

Fig. 9. Stochastic reconstructed models based on the 3D morphological description curve from the micro-X-ray CT model.

Table 1
Difference between the morphological description obtained from surface images and that of the micro-X-ray CT model.

Ω	Image A	Image B	Image C	Image D
Method 1	0.00025	0.00090	0.00030	0.00034
Method 2	0.00050	0.00090	0.00026	0.00030

two curves, an error index is defined

$$Err = \frac{Max\ |CT - \text{reconstructed}|}{Max(CT)} \times 100\% \quad (25)$$

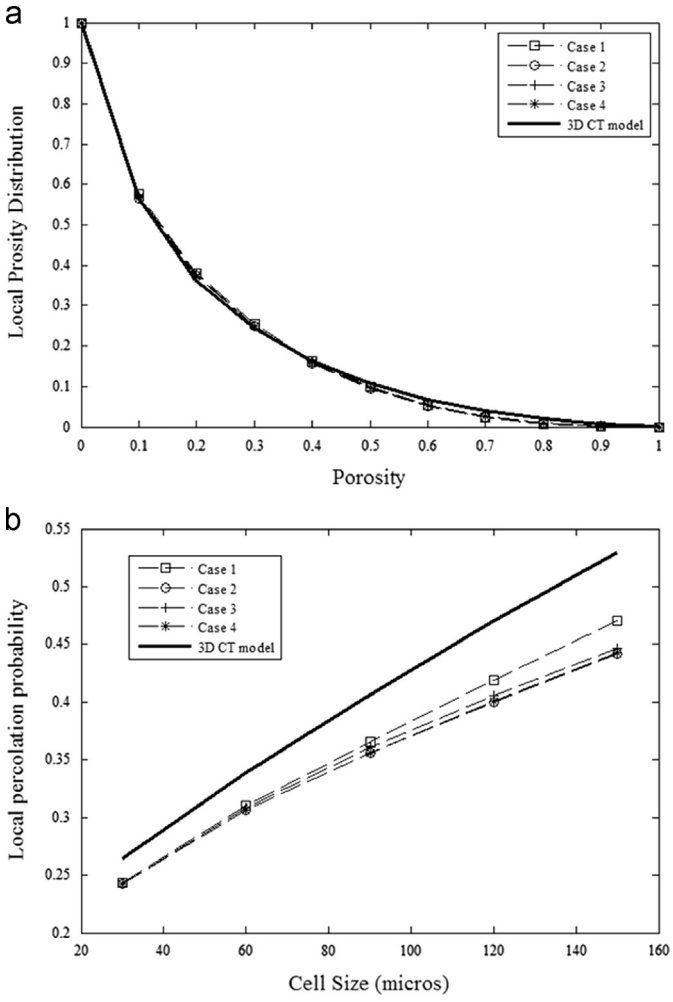

Fig. 10. Quantitative measures of the reconstructed models based on the X-ray micro-CT model. (a) Local porosity distribution at cell side length of 180 micros and (b) local percolation probability.

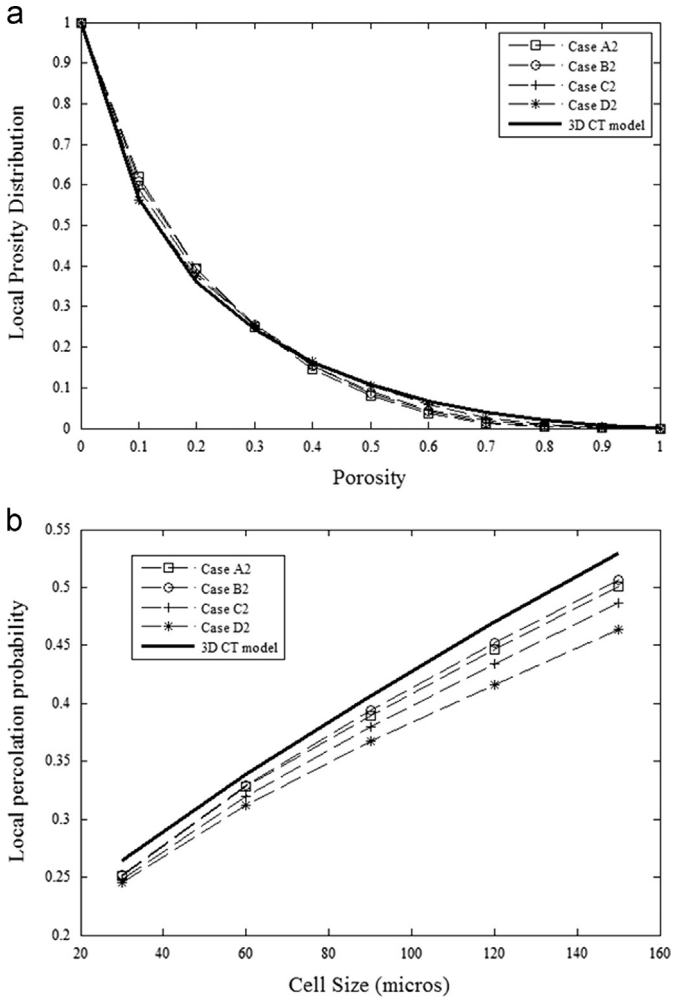

Fig. 11. Quantitative measures of the reconstructed models based on the surface images. (a) Local porosity distribution at cell side length of 180 micros and (b) local percolation probability.

Table 2
Quantitative morphological description of the stochastic reconstructed models based on the micro-X-ray CT model.

Case no.	Specific area Err (%)	Local porosity distribution Err (%)	Local percolation probability Err (%)
1	5	2.07	11.13
2	5	1.59	16.48
3	5	1.64	15.59
4	5	1.19	16.26
Average	5	1.62	14.87

Results of the error analysis are listed in Table 2. It can be seen that, the morphological measurements of these reconstructed models are close to the X-ray micro-CT model.

5.2. *Reconstruction based on the surface images*

In this section, the derived morphological distribution curves from the surface images captured by the digital microscopy are used. Fig. 11 shows the local porosity distribution and local percolation probability of reconstructed models using method 2. It shows that the reconstructed microstructure models based on the surface images can also give reasonably good results. The results of error analysis performed on the reconstructed models from 4 surface images based on method 1 and method 2 are listed in Table 3. The average error of the local porosity distribution at cell side length of 180 μm is reported as less than 4%, and a error of around 10% is presented in the measurement of local percolation probability, which shows the effectiveness of stochastic reconstruction from surface images. In practice, the specific area can be an input value, obtained from other experiments. If the specific area is given, the distribution curve from surface images that gives the best fit can be used in the stochastic reconstruction (case D of this example).

Table 3
Quantitative morphological description of the stochastic reconstructed model based on the surface images by using method 1 and method 2 ("A, B, C, D" refers to id of the surface image in Fig. 8, "1" and "2" represent method 1 and method 2 respectively).

Case no.	Specific area		Local porosity distribution		Local percolation probability	
	Err (%)	Average	Err (%)	Average	Err (%)	Average
A1	23.51	20.09	3.74	3.07	7.05	10.50
B1	33.19		5.75		5.96	
C1	13.31		1.62		15.00	
D1	10.35		1.17		14.00	
A2	30.82	24.12	5.56	3.50	5.37	7.53
B2	31.86		4.45		4.33	
C2	21.05		2.53		7.98	
D2	12.76		1.47		12.45	

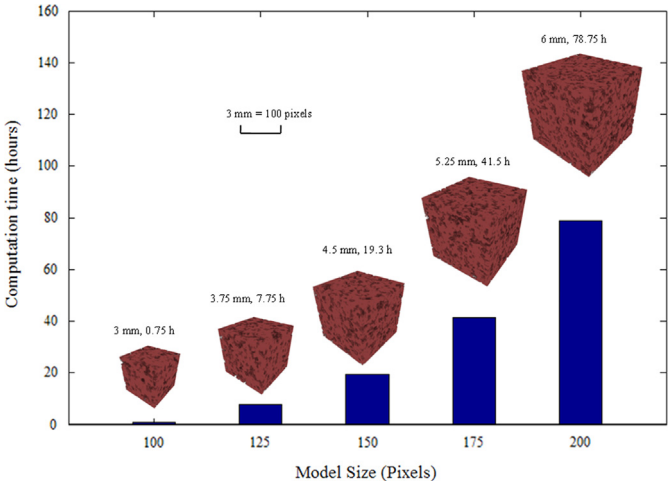

Fig. 12. Computational time of reconstructed models with different sizes.

It should be mentioned that the Representative Element Volume (REV) of the Gosford sandstone for the stochastic reconstruction is smaller than a cube with size of 600 pixels (3 mm). The stochastic reconstruction is also used to generate models with size of $3.75 \times 3.75 \times 3.75\ mm^3$, $4.5 \times 4.5 \times 4.5\ mm^3$, $5.25 \times 5.25 \times 5.25\ mm^3$ and $6 \times 6 \times 6\ mm^3$. In our test, a computer with Intel Core i7 960 3.20 GHz and memory of 8 GB is used. The program runs in a 64-bit version of Windows 7 with Matlab 2012. The reconstructed models and the corresponding simulation time are summarized in Fig. 12. This example demonstrates the capability of stochastic reconstruction in reproducing models of arbitrary large size with only a small observation domain. However, the computational requirement is demanding when the model size becomes large. This issue will be addressed in future research.

6. Conclusions

The stochastic reconstruction of Gosford sandstone from its surface image is conducted. A digital microscope is adopted to capture surface images of the Gosford sandstone specimen where the carbon dust treatment on the surface is introduced. The 3D morphological distribution curve is derived through a porosity adjustment of the 2D surface images. It is found that the derived morphological curves are close to that from the X-ray micro-CT model. By comparing all the stochastic reconstructed microstructure models with the original X-ray micro-CT model, it is shown that the reconstructed models can successfully reflect essential morphological information of Gosford sandstone.

Acknowledgments

This research is financially supported by the Australian Research Council (Grant no. DE130100457).

References

[1] Adler PM, Jacquin CG, Quiblier JA. Flow in simulated porous media. Int J Multiph Flow 1990;16(4):691–712.
[2] Hazor YH, Zur A, Mimran Y. Microstructure effects on microcracking and brittle failure of dolomites. Tectonophysics 1997;281(3):141–61.
[3] Ichikawa Y, Kawamura K, Uesugi K, Seo YS, Fujii N. Micro- and macro behavior of granitic rock: observations and viscoelastic homogenization analysis. Comput Methods Appl Mech Eng 2001;191:47–72.
[4] Wang XS, Wu BS, Wang QY. Online SEM investigation of microcrack characteristics of concretes at various temperatures. Cem Concr Res 2005;35:1385–90.
[5] Josh M, Esteban L, DellePiane C, Sarout J, Dewhurst DN, Clennell MB. Laboratory characterisation of shale properties. J Pet Sci Eng 2012;88–89:107–24.
[6] Sufian A, Russell AR. Microstructural pore changes and energy dissipation in Gosford sandstone during pre-failure loading using X-ray CT. Int J Rock Mech Min Sci 2013;57:119–31.
[7] Hazlett RD. Statistical characterization and stochastic modeling of pore networks in relation to fluid flow. Math Geol 1997;29(6):801–22.
[8] Torquato CLY, Torquato S. Reconstructing random media. Phys Rev E 1998;57(1):495–506.
[9] Torquato CLY, Torquato S. Reconstructing random media. II. Three-dimensional media from two-dimensional cuts. Phys Rev E 1998;58(1):224–33.
[10] Okabe H, Blunt MJ. Pore space reconstruction using multiple-point statistics. J Pet Sci Eng 2005;46(1–2):121–37.
[11] Politis MG, Kikkinides ES, Kainourgiakis ME, Stubos AK. A hybrid process-based and stochastic reconstruction method of porous media. Microporous Mesoporous Mater 2008;110(1):92–9.
[12] Hajizadeh A, Safekordi A, Farhadpour FA. A multiple-point statistics algorithm for 3D pore space reconstruction from 2D images. Adv Water Resour 2011;34(10):1256–67.
[13] Tahmasebi P, Sahimi M. Reconstruction of three-dimensional porous media using a single thin section. Phys Rev E 2012;85(6):066709.
[14] Rintoul MD, Torquato S. Reconstruction of the structure of dispersions. J Colloid Interface Sci 1997;186(2):467–76.
[15] Manwart C, Torquato S, Hilfer R. Stochastic reconstruction of sandstones. Phys Rev E 2000;62(1):893–9.
[16] Talukdar MS, Torsaeter O. Reconstruction of chalk pore networks from 2D backscatter electron micrographs using a simulated annealing technique. J Pet Sci Eng 2002;33(4):265–82.
[17] Jiao Y, Stillinger FH, Torquato S. Modeling heterogeneous materials via two-point correlation functions. II. Algorithmic details and applications. Phys Rev E 2008;77(3):031135.
[18] Talukdar MS, Torsaeter O, Ioannidis MA, Howard JJ. Stochastic reconstruction of chalk from 2D images. Transp Porous Media 2002;48(1):101–23.
[19] Talukdar MS, Torsaeter O, Ioannidis MA, Howard JJ. Stochastic reconstruction, 3D characterization and network modeling of chalk. J Pet Sci Eng 2002;35(1–2):1–21.
[20] Ouenes A., Bhagavan S., Bunge P.H., Travis B.J. Application of simulated annealing and other global optimization methods to reservoir description: myths and realities. In: Proceedings of the SPE(28415) paper, 1994.
[21] Hilfer R. Local porosity theory and stochastic reconstruction for porous media. Statistical physics and spatial statistics. Berlin: Springer; 2000; 203–41.
[22] Øren PE, Bakke S. Reconstruction of Berea sandstone and pore-scale modelling of wettability effects. J Pet Sci Eng 2003;39(3–4):177–99.